

In-situ High-energy X-ray Study of Deformation Mechanisms in Additively Manufactured 316 Stainless Steel

Xuan Zhang*, Meimei Li*, Jun-Sang Park*, Peter Kenesei*, Jonathan Almer*

*Argonne National Laboratory, 9700 S Cass Ave, Lemont IL 60525
xuanzhang@anl.gov

INTRODUCTION

The key structural material in the core of the Transformational Challenge Reactor is the additively manufactured 316L stainless steel (AM 316L). Therefore, its deformation mechanism in service conditions must be understood. Previous studies have shown that the AM 316L possesses an outstanding balance of strength and ductility due to the unique hierarchical microstructure [1] or texture [2]. In this work, the room temperature tensile deformation of AM 316L SS was studied by *in-situ* high-energy x-ray diffraction and x-ray tomography/radiography techniques at the Advanced Photon Source (APS) in Argonne National Laboratory. The lattice strain evolution, the dislocation kinetics, and the coherent domain size evolution during the deformation process was monitored. The morphology of the pores in the AM 316L during deformation was tracked.

MATERIAL AND METHOD

SS J3-type tensile samples made out of AM 316L were provided by Oak Ridge National Laboratory under the Transformation Challenge Reactor program. The AM 316L build was fabricated by a laser powder bed fusion process using a GE Concept Laser-M2 printer [3]. The sample had a gage length of 5 mm and a cross section of 0.79 mm \times 1.19 mm, measured by x-ray radiography. The tensile tests were performed at room temperature in air using a μ TS load frame manufactured by Psylotech Inc., at the beamline 1-ID of the APS. The strain rate was 5E-5 /s for the first few percent of strain, and then changed to 2E-4 /s for the rest of the test. No strain rate sensitivity was expected at room temperature. During the tensile test, monochromatic x-ray beams transmitted through the sample around the center of the gage, and the diffraction signal was received by a GE RT-41 area detector 881 mm down-stream from the sample. The x-ray energy was 80.725 keV and the beam size was 30 μ m \times 40 μ m. For the AM 316L sample, tensile deformation and diffraction measurements were paused at 5 intermittent steps for x-ray tomography. Except for the last scan, which was around the necking center (the necking center was not at the gage center in this sample), the other 4 scans were all centered on the gage, giving a direct observation of the change of morphology of a group of pores. The beam size for tomography was 2.0 mm (W) \times 1.0 mm (L).

The x-ray diffraction data was processed by a MatLab package provided by the beamline. The area detector signals were first converted to 1-dimensional (1-D) diffraction profiles in the loading direction by summing up the intensities of each Debye-Scherrer ring from $\pm 10^\circ$ around the loading direction, and the peaks were fitted for peak positions to obtain the lattice strain as a function of tensile strain in the loading direction. The entire area detector signals were then processed and fitted to obtain the full-width at half-maximum (FWHM) using a method detailed in [4]. The FWHM data was analyzed using the modified Williamson-Hall (W-H) method [5] to obtain the evolution of dislocations and coherently scattering domain sizes with deformation,. Details of the FWHM data analysis method can be found in [4].

RESULTS AND SUMMARY

Fig. 1 shows the stress-strain (s-s) curve of the AM316L sample. The scatter plot is the engineering s-s curve, and the line is the true s-s curve. The true stress-strain curve is only up to the ultimate tensile strength (UTS). It shows a yield strength (YS) of 423 MPa, a UTS of 590 MPa, and a total elongation (ϵ_u) of 66.4%.

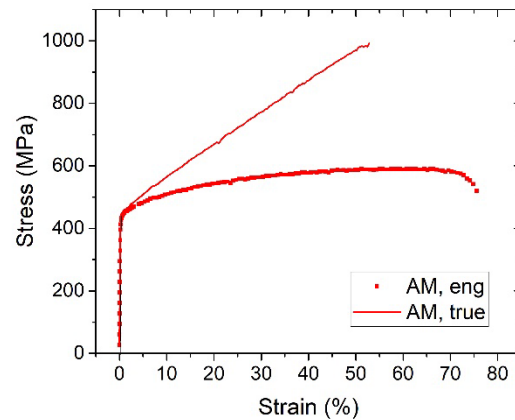


Fig. 1. Room temperature stress-strain curves of the conventional 316L and the AM 316L tested in this work.

Fig. 2 shows the lattice strain (left) and the FWHM (right) as a function of true strain, for the 3rd to the 9th peaks of the face-centered cubic (FCC) AM 316L. Those parameters all increase monotonically with strain. The FWHM data are analyzed by the modified W-H method to gain insights into the dislocation dynamics, and the behavior of AM 316L will be compared with that of the

conventional 316L to understand the differences in their tensile behavior.

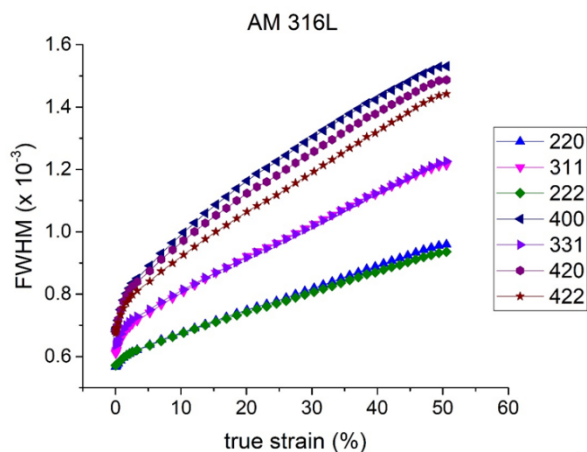
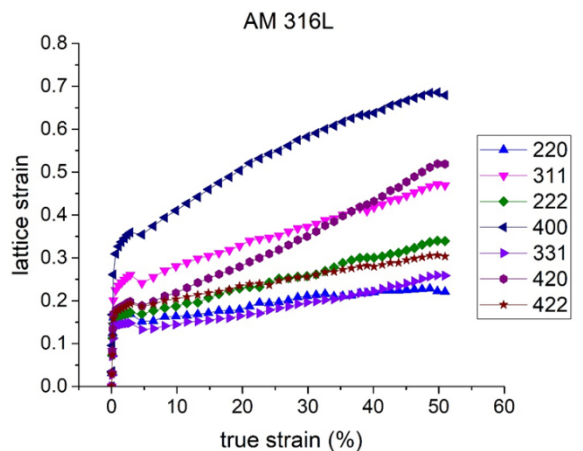


Fig. 2. The lattice strain (left) and the FWHM (right) as a function of true strain, for the 3rd to the 9th peaks of the AM 316L sample.

The x-ray radiographs taken from the gage center of AM316L (Fig. 3) reveal the internal porosity within the sample. The as-received sample has a high density of spherical pores ranging from sub- μm to $\sim 50 \mu\text{m}$, together with a low density of larger, irregular-shaped pores. The radiographs at different strains show that the pores become elongated with increasing tensile deformation. As necking progresses, cracks initiated at a few large pores near the specimen edge.

Further analysis of synchrotron high-energy x-ray diffraction and tomography/radiography is being conducted to understand the deformation mechanism in AM 316L stainless steel.

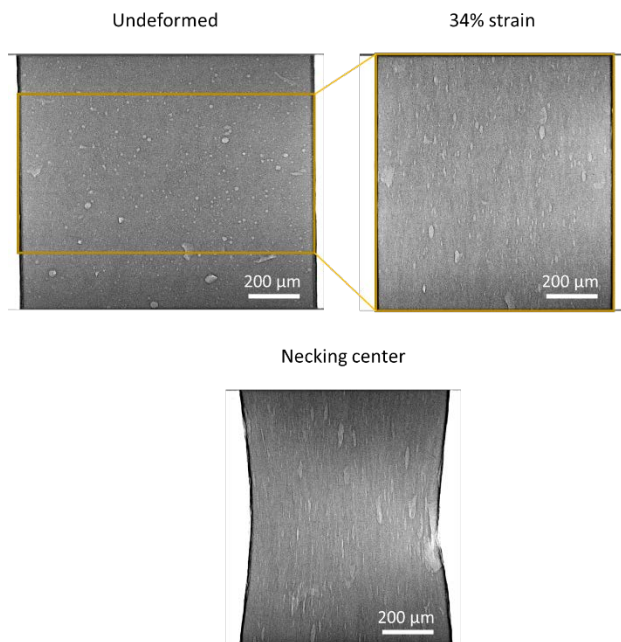


Fig. 3. X-ray radiographs of the gage area of AM 316L showing the internal porosity at different deformation levels.

ACKNOWLEDGEMENT

Work was supported by the Transformational Challenge Reactor Program supported by the U.S. Department of Energy, Office of Nuclear Energy under Contract DE-AC02-06CH11357. AM materials were provided by Oak Ridge National Laboratory. This research used resources of the Advanced Photon Source, a U.S. Department of Energy (DOE) Office of Science User Facility operated for the DOE Office of Science by Argonne National Laboratory under Contract No. DE-AC02-06CH11357. We would like to thank Yiren Chen and Hoon Lee for assistance with the sample preparation and the APS experiment.

REFERENCES

- [1] Y.M. WANG, T. VOISIN, J.T. MCKEOWN, J. YE, N.P. CALTA, Z. LI, Z. ZENG, Y. ZHANG, W. CHEN, T.T. ROEHLING, R.T. OTT, M.K. SANTALA, PHILIP J. DEPOND, M.J. MATTHEWS, A.V. HAMZA, T. ZHU, Additively manufactured hierarchical stainless steels with high strength and ductility, *Nature Materials* **17**(1) (2018) 63-71.
- [2] Z. SUN, X. TAN, S.B. TOR, C.K. CHUA, Simultaneously enhanced strength and ductility for 3D-printed stainless steel 316L by selective laser melting, *NPG Asia Materials* **10**(4) (2018) 127-136.
- [3] K. FIELD, J. SIMPSON, M. GUSSEV, H. WANG, M. LI, X. ZHANG, X. CHEN, T. KOYANAGI, K. KANE, A.

MARQUEZ ROSSY, M. BALOOCH, K. TERRANI, Handbook of Advanced Manufactured Material Properties from TCR Structure Builds at ORNL - FY 2019, Oak Ridge National Laboratory, 2019.

[4] X. ZHANG, M. LI, J.-S. PARK, P. KENESEI, J. ALMER, C. XU, J.F. STUBBINS, In situ high-energy X-ray diffraction study of tensile deformation of neutron-irradiated polycrystalline Fe-9%Cr alloy, *Acta Materialia* **126** (2017) 67-76.

[5] T. UNGÁR, A. BORBÉLY, The effect of dislocation contrast on x-ray line broadening: A new approach to line profile analysis, *Applied Physics Letters* **69**(21) (1996) 3173-3175.